Polymer Chemistry

Accepted Manuscript

This is an *Accepted Manuscript*, which has been through the Royal Society of Chemistry peer review process and has been accepted for publication.

Accepted Manuscripts are published online shortly after acceptance, before technical editing, formatting and proof reading. Using this free service, authors can make their results available to the community, in citable form, before we publish the edited article. We will replace this *Accepted Manuscript* with the edited and formatted *Advance Article* as soon as it is available.

You can find more information about *Accepted Manuscripts* in the Information for Authors.

Please note that technical editing may introduce minor changes to the text and/or graphics, which may alter content. The journal's standard Terms & Conditions and the Ethical guidelines still apply. In no event shall the Royal Society of Chemistry be held responsible for any errors or omissions in this *Accepted Manuscript* or any consequences arising from the use of any information it contains.

ROYAL SOCIETY OF CHEMISTRY

www.rsc.org/polymers

Polymer Chemistry

RSCPublishing

ARTICLE

Modification of block copolymer vesicles: What will happen when AB diblock copolymer is block-extended to ABC triblock terpolymer?

Cite this: DOI: 10.1039/x0xx00000x

Received 00th January 2012,
Accepted 00th January 2012

DOI: 10.1039/x0xx00000x

www.rsc.org/

Xiaoyan Shen,[a] Fei Huo,[b] Haijiao Kang,[a] Shifeng Zhang,[*,a] Jianzhang Li,[*,a] and Wangqing Zhang[*,b]

ABSTRACT: Well-defined vesicles of poly(ethylene glycol)-*block*-polystyrene (PEG-*b*-PS) were prepared through the macro-RAFT agent mediated dispersion polymerization, and modification of the PEG-*b*-PS vesicles by the extension of the third solvophilic poly(4-vinylpyridine) block through seeded RAFT polymerization was investigated. It was found, during the seeded RAFT polymerization, the PEG-*b*-PS diblock copolymer was extended to the poly(ethylene glycol)-*block*-polystyrene-*block*-poly(4-vinylpyridine) (PEG-*b*-PS-*b*-P4VP) triblock terpolymer, and the PEG-*b*-PS vesicles were converted into the membrane-compartmentalized PEG-*b*-PS-*b*-P4VP vesicles (MCVs), in which the poly(4-vinylpyridine) chains were found to be uniformly distributed in the inner side of the membrane, whereas at the outer side of the membrane several poly(4-vinylpyridine) chains were converged together and were segregated by the neighbouring poly(ethylene glycol) chains. The proposed seeded RAFT polymerization may be a promising method of vesicle modification, and the MCVs with segregated membrane structure are deemed to be a new morphology of the block copolymer nano-assemblies.

1 Introduction

Block copolymer vesicles, which have enclosed bilayer structure with the solvophobic block forming the membrane and the solvophilic block locating at both the inner and outer sides of the membrane, have attracted increasing interest in recent years, since these block copolymer vesicles have numerous applications such as tunable delivery vehicles.[1-2] In these years, benefited from a large quantity of block copolymers and the tunable preparation procedures, various vesicles such as the general bilayer vesicles,[3-14] unilamellar vesicles,[15,16] multilayer vesicles,[17,18] spotted vesicles,[19] mesh-like vesicles[20,21,] and large compound vesicles[22,23] have been reported. Summarily, there exists two methods to prepare block copolymer vesicles. The first is through self-assembly of amphiphilic block copolymers in the block selective solvent.[4-18] Following this self-assembly strategy, an amphiphilic block copolymer with suitable composition is initially dissolved in a common solvent, and then a block selective solvent is added, and finally the common solvent is removed usually by dialysis to afford the micelles kinetically frozen in the block selective solvent. This strategy suffers from the inconvenience of multi procedures being included and the disadvantage of diluted block copolymer concentration usually below 1%. Recently, the *in situ* synthesis of block copolymer nano-objects by polymerization-induced self-assembly (PISA) especially through the macromolecular RAFT (macro-RAFT) agent mediated dispersion polymerization seems very reliable, since it affords convenient *in situ* synthesis of block copolymer nano-objects including vesicles.[24-36] Following this PISA, the controlled radical polymerization, *e.g.* RAFT polymerization mediated with a macro-RAFT agent at most cases,[27-36] under dispersed condition is performed, and the *in situ* synthesis of block copolymer nano-objects is achieved. This PISA strategy has the advantages of the *in situ* synthesis of concentrated block copolymer nano-objects with polymer concentration up to 30% and the tunable morphology of the block copolymer nano-objects just by increasing the monomer conversion in the RAFT polymerization.

Generally, the size and morphology of block copolymer vesicles are determined by the size of the solvophobic block relative to the solvophilic block in the amphiphilic block copolymer.[37] It is deemed that the amphiphilic block copolymer with the packing parameter p at $1/2 \leq p \leq 1$ favors formation of vesicles in the block selective solvent.[38] For block copolymer vesicles under non-equilibrium state,[37] the size and morphology of block copolymer vesicles depend less on thermodynamics and more on non-equilibrium aspects of the formation process such as the block copolymer concentration and the solvent character, which is the reason that block copolymer vesicles with various morphologies such as tubules,[39,40] oblates[41,42] and starfish[43] have reported. This suggests that modification of block copolymer vesicles can be achieved by either changing the solvophobic/solvophilic ratio in the block copolymer or the formation process. However, these two ways to change/modify block

Polymer Chemistry Accepted Manuscript

copolymer vesicles suffer somewhat incontinence or are out of control in the vesicle morphology. For examples, changing the composition of block copolymer may lead to formation of block copolymer nano-objects other than block copolymer vesicles.

Seeded polymerization is a convenient method to synthesize polymeric nano-objects.[44] By employing the reversible addition-fragmentation chain transfer (RAFT) polymerization technology in seeded polymerization,[45-49] the polymer chains tethered onto the seeds are block-extended with the monomer conversion, and the size or morphology of the seeds changes with the block-extension, and therefore modification of the block copolymer nano-objects is achieved. In this contribution, we propose a strategy to modify vesicles of AB diblock copolymer by inserting a new solvophilic C block at the end of the solvophobic B block through seeded RAFT polymerization. It is found, during the seeded RAFT polymerization, the poly(ethylene glycol)-*block*-polystyrene (PEG-*b*-PS) diblock copolymer was converted into the poly(ethylene glycol)-*block*-polystyrene-*block*-poly(4-vinylpyridine) (PEG-*b*-PS-*b*-P4VP) triblock terpolymer, and the PEG-*b*-PS vesicles were modified into the PEG-*b*-PS-*b*-P4VP vesicles containing a compartmentalized membrane, which were called membrane-compartmentalized vesicles (MCVs). The proposed seeded RAFT polymerization may be a promising method of vesicle modification, and the MCVs may be one of new morphology of the block copolymer nano-assemblies.

2 Experimental

2.1 Materials

The monomers of 4-vinylpyridine (4VP, 96%, Alfa) and styrene (St, >98%, Tianjin Chemical Company) were distilled under reduced pressure prior to use. The macromolecular RAFT (macro-RAFT) agent of poly(ethylene glycol) trithiocarbonate (PEG_{45}-TTC, in which TTC represents the RAFT terminal of trithiocarbonate) was prepared by esterification reaction of the hydroxy terminal in the monohydroxyl-terminated poly(ethylene glycol) of *m*PEG_{45}-OH with the carboxyl group in the trithiocarbonate of *S*-1-dodecyl-*S*′-(α,α′-dimethyl-α″-acetic acid)[50] as described elsewhere.[51] 2,2'-Azobis(isobutyronitrile) (AIBN, >99%, Tianjin Chemical Company, China) was recrystallized from ethanol before being used. All other chemical reagents with analytical grade were purified by standard procedures or used as received. Deionized water was used.

2.2 Preparation of the PEG-*b*-PS-TTC vesicles

The vesicles of the diblock copolymer of poly(ethylene glycol)-*b*-polystyrene trithiocarbonate (PEG-*b*-PS-TTC) were prepared through the *in situ* synthesis strategy of the PEG_{45}-TTC macro-RAFT agent mediated dispersion polymerization of styrene in the methanol/water mixture (80/20, w/w) as discussed elsewhere.[36] Into a 250 mL round-bottomed flask with a magnetic bar, PEG_{45}-TTC (1.13 g, 0.481 mmol), St (15.0 g, 14.4 mol), AIBN (0.0263 g, 0.160 mmol), and the methanol/water mixture (100.00 g, 80/20 by weight) were added. The flask content was degased with nitrogen at 0 ℃ to remove oxygen, and then the flask was sealed and immersed into the preheated oil bath at 70 ℃ to initiate the RAFT polymerization. After 24 h, the polymerization was quenched by rapid cooling upon immersing the flask into ice-water, and the monomer conversion at 92.7% was determined by UV-vis analysis at 245 nm as discussed elsewhere.[52] The colloidal dispersion of the PEG-*b*-PS-TTC vesicles was dialyzed against the 80/20 methanol/water mixture (250 mL × 3) to remove the residual monomer of styrene. After removal of the residual monomer, the PEG-*b*-PS-TTC vesicles dispersed in the 80/20 methanol/water mixture with the polymer concentration at 17.0 wt% were kept at room temperature for the next use.

2.3 Vesicle modification by seeded RAFT polymerization

Into a 50 mL Schlenk flask with a magnetic bar, the PEG-*b*-PS-TTC vesicles dispersed in the 80/20 methanol/water mixture (3.513 g, containing 0.0190 mmol of PEG_{45}-*b*-PS_{278}-TTC), 4VP (0.30 g, 2.86 mmol), and the initiator of AIBN (10.40 mg, 0.0635 mmol) dissolved in the 80/20 methanol/water mixture (0.668 g) was added. The flask content was vigorously stirred for 10 min, degassed with nitrogen at 0 ℃, and then the polymerization was initiated by immersing the flask into preheated oil bath at 70 ℃. After a given time, the polymerization was quenched by immersing the flask in ice-water, and the monomer conversion was detected by ^{1}H NMR analysis, and the morphology of the *in situ* synthesized nano-objects of the PEG-*b*-PS-*b*-P4VP triblock terpolymer was checked by transmission electron microscope (TEM). To collect the PEG-*b*-PS-*b*-P4VP triblock terpolymer, the PEG-*b*-PS-*b*-P4VP nano-objects were separated by centrifugation (12500 r/min, 10 min), then washed twice with *n*-hexane, and finally dried at room temperature under vacuum to afford the triblock terpolymer.

2.4 Characterization

The ^{1}H NMR analysis was performed on a Bruker Avance III 400MHz NMR spectrometer using $CDCl_3$ as the solvent. The UV-vis analysis was performed on a Varian 100 UV-vis spectrophotometer. The molecular weight and the polydispersity index (PDI, PDI = M_w/M_n) were determined by using a Viscotek GPC Max Ve2001 solvent/sample module equipped with a DAWN HELEOS 8 light scattering photometer, a ViscoStar viscometer, and an Optilab rEX interferometric refractometer from Wyatt Technology Corporation. Samples were passed through three Mz-Gel SD plus 10 μm columns using DMF as eluent at flow rate of 1.0 mL/min with narrowly polydispersed polystyrene as calibration standard. The conversion of the 4VP monomer in the seeded RAFT polymerization was detected by ^{1}H NMR analysis, in which a drop of the polymerization solution (about 0.05 mL) was diluted with $CDCl_3$ (0.5 mL) and subjected to ^{1}H NMR analysis to determine the monomer conversion. The TEM observation was performed using a Tecnai G^2 F20 electron microscope at an acceleration of 200 kV. To detect the morphology of the PEG-*b*-PS-*b*-P4VP triblock terpolymer nano-objects, a small drop of the colloids dispersed in the polymerization medium of the 80/20 methanol/water mixture (~0.01 mL) was added in water (1 mL), and then a small drop of the diluted dispersion was dripped onto a piece of copper grid covered with thin film of carbon, dried at room temperature, and finally observed by TEM. For the typical PEG_{45}-*b*-PS_{278}-*b*-$P4VP_{105}$ nano-objects, three different TEM sampling procedures for the unstained nano-objects, the nano-objects stained by I_2 vapor, and the nano-objects jointly stained by phosphotungstic acid (PTA) and I_2 vapor were adopted,

Polymer Chemistry Accepted Manuscript

 This journal is © The Royal Society of Chemistry 2012

respectively. For the unstained nano-objects, a small drop of the diluted colloidal dispersion was dripped onto a piece of copper grid, dried at room temperature till the solvent was evaporated; for the nano-objects stained by I_2 vapor, a small drop of the diluted colloidal dispersion was dripped onto a piece of copper grid, dried at room temperature, stained by I_2 vapor at 50 ^{0}C for 30 min under reduced pressure; for the nano-objects jointly stained by PTA and I_2 vapor, into the diluted dispersion of the PEG_{45}-*b*-PS_{278}-*b*-$P4VP_{105}$ nano-objects (1 mL), a drop of 1.5 wt% PTA aqueous solution (~0.01 mL) was added, kept at room temperature for 2 min, and then a small drop of the colloids was dripped onto a piece of copper grid, dried at room temperature, and then stained by I_2 vapor at 50 ^{0}C for 30 min under reduced pressure, and finally observed by TEM.

3 Results and discussion

3.1 Preparation of the PEG-*b*-PS-TTC vesicles

The PEG_{45}-*b*-PS_{278}-TTC vesicles were prepared through the PEG_{45}-TTC macro-RAFT agent mediated dispersion polymerization of styrene in the 80/20 methanol/water mixture under $[St]_0$:$[PEG_{45}\text{-}TTC]_0$:$[AIBN]_0$ = 900:3:1 with the weight ratio of fed monomer to the solvent at 15% as shown in Scheme 1. This synthesis strategy was chosen, since it afforded a continent *in situ* synthesis of the PEG-*b*-PS-TTC vesicles as discussed elsewhere.[36] After 24 h polymerization, 92.7% monomer conversion was obtained, and the *in situ* synthesis of the PEG_{45}-*b*-PS_{278}-TTC vesicles were achieved. The synthesized PEG_{45}-*b*-PS_{278}-TTC vesicles can be easily dispersed in the 80/20 methanol/water mixture with the polymer concentration at 17.0 wt%. It is found that, after kept in a glass flask at room temperature for about 2 month, just fewer amount of precipitate is observed at the flask bottom. After a gentle stirring, the precipitate can be re-dispersed in the solvent of the 80/20 methanol/water mixture.

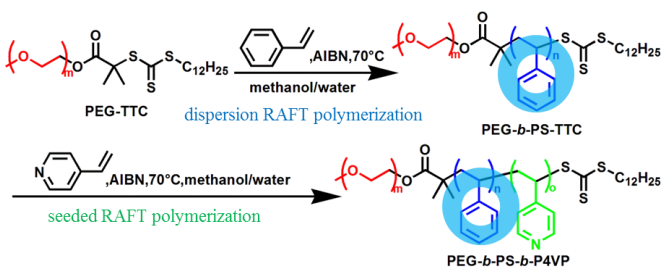

Scheme 1. Synthesis of the PEG-*b*-PS-TTC vesicles by dispersion RAFT polymerization and the vesicle modification by seeded RAFT polymerization.

Figure 1A shows the TEM images of the PEG_{45}-*b*-PS_{278}-TTC vesicles, from which vesicles with the size from 120 to 190 nm have been discerned. In the 80/20 methanol/water mixture, the PEG block is soluble and the PS block is insoluble, and therefore the PS block forms the membrane of vesicles and the PEG chains are tethered on the inner and outer sides of the membrane as shown in Figure 1B. Despite the size of the PEG_{45}-*b*-PS_{278}-TTC vesicles is not very uniform, it is found that the membrane thickness of 27 ±3 nm, which is calculated by statistical analysis of above 100 vesicles, of the PEG_{45}-*b*-PS_{278}-TTC vesicles is very close to each other. Besides, based on the DP of the PS block, the maximum length L_{max} of the extended molecular chain of the PS_{278} block, 35 nm, is calculated, which is about 1.3 times of the membrane thickness, and therefore the bilayer structure of the PEG_{45}-*b*-PS_{278}-TTC vesicles with the RAFT terminal embedded in the membrane as shown in Figure 1B is confirmed.

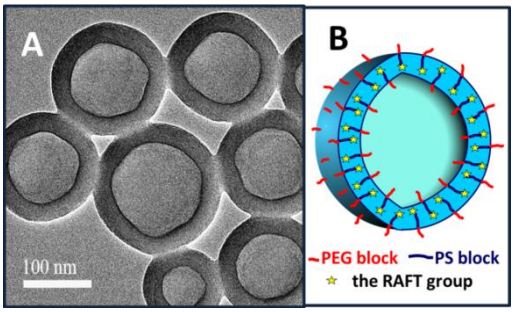

Figure 1. The TEM image (A) and the schematic structure (B) of the PEG_{45}-*b*-PS_{278}-TTC vesicles.

The polymer constructed with the PEG_{45}-*b*-PS_{278}-TTC vesicles was characterized by GPC analysis (Figure 2) and ^{1}H NMR analysis (Figure 3). From the GPC traces, the molecular weight of PEG_{45}-*b*-PS_{278}-TTC, $M_{n,GPC}$, at 24.3 kg/mol and the low PDI at 1.07 comparable to that of the PEG_{45}-TTC macro-RAFT agent was obtained. By checking the ^{1}H NMR spectra of PEG_{45}-*b*-PS_{278}-TTC with its precursor of the PEG_{45}-TTC macro-RAFT agent, formation of the PEG-*b*-PS-TTC diblock copolymer is confirmed. By comparing the proton resonance signals at δ = 6.26-7.23 ppm (*f*, *g*, *h*) ascribed to the phenyl group in PS block and δ = 3.64 ppm (*b*) ascribed to the PEG backbone, the polymer molecular weight $M_{n,NMR}$ of the synthesized PEG_{45}-*b*-PS_{278}-TTC at 33.7 kg/mol is calculated. Clearly, $M_{n,GPC}$ of the synthesized PEG_{45}-*b*-PS_{278}-TTC is lower than $M_{n,NMR}$, and the reason is possibly due to the PS standard used in the DMF-based GPC analysis. It is found that $M_{n,NMR}$ of the synthesized PEG_{45}-*b*-PS_{278}-TTC is very close to the theoretical weight ($M_{n,th}$) at 31.3 kg/mol, which is calculated by the monomer conversion following equation 1 as discussed elsewhere,[53] and therefore the high block efficiency at about 100% in the dispersion RAFT polymerization is confirmed.

$$M_{n,th} = \frac{[\text{monomer}]_0 \times M_{monomer}}{[\text{RAFT}]_0} \times Conversion + M_{RAFT} \quad (1)$$

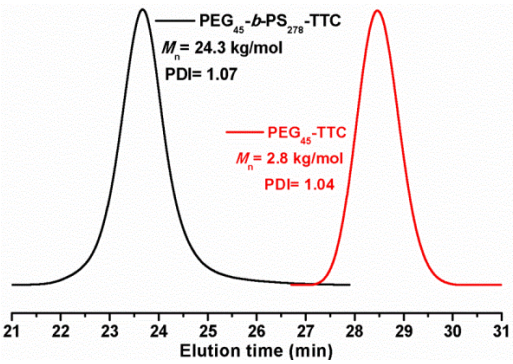

Figure 2. GPC traces of PEG_{45}-TTC and PEG_{45}-*b*-PS_{278}-TTC.

Polymer Chemistry Accepted Manuscript

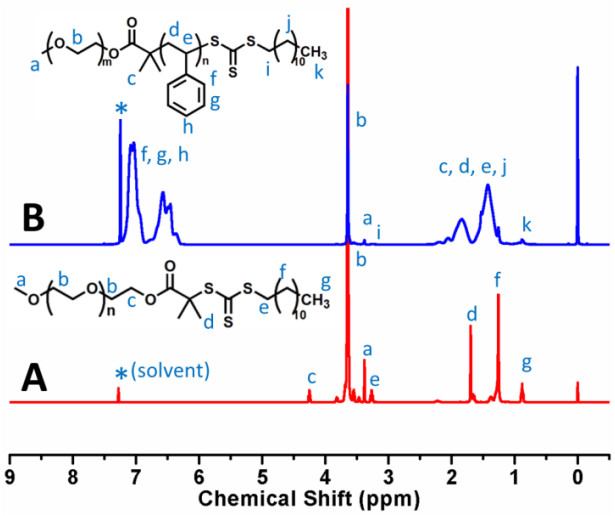

Figure 3. The ^{1}H NMR spectra of PEG_{45}-TTC (A) and PEG_{45}-*b*-PS_{278}-TTC (B).

3.2 Seeded RAFT polymerization and the vesicle evolution

Since the RAFT terminal is embedded with the vesicles membrane, the third P4VP block can be inserted onto the vesicle membrane through seeded RAFT polymerization as shown in Scheme 1. The seeded RAFT polymerization of 4VP is carried out in the 80/20 methanol/water mixture under $[4VP]_0$:$[PEG_{45}$-*b*-PS_{278}-$TTC]_0$:$[AIBN]_0$ = 450:3:1. In the 80/20 methanol/water mixture, both the fed monomer 4VP and the newly formed third block P4VP are soluble, and therefore the present seeded RAFT polymerization looks like a typical homogeneous RAFT polymerization. With the progress of the seeded RAFT polymerization, the third block P4VP extends, the vesicles were modified and converted into the PEG-*b*-PS-*b*-P4VP triblock terpolymer nano-objects. Clearly, the present seeded RAFT polymerization is somewhat like the graft-through strategy discussed elsewhere,[54] since a new polymer chain is block-extended or formed in the two methods.

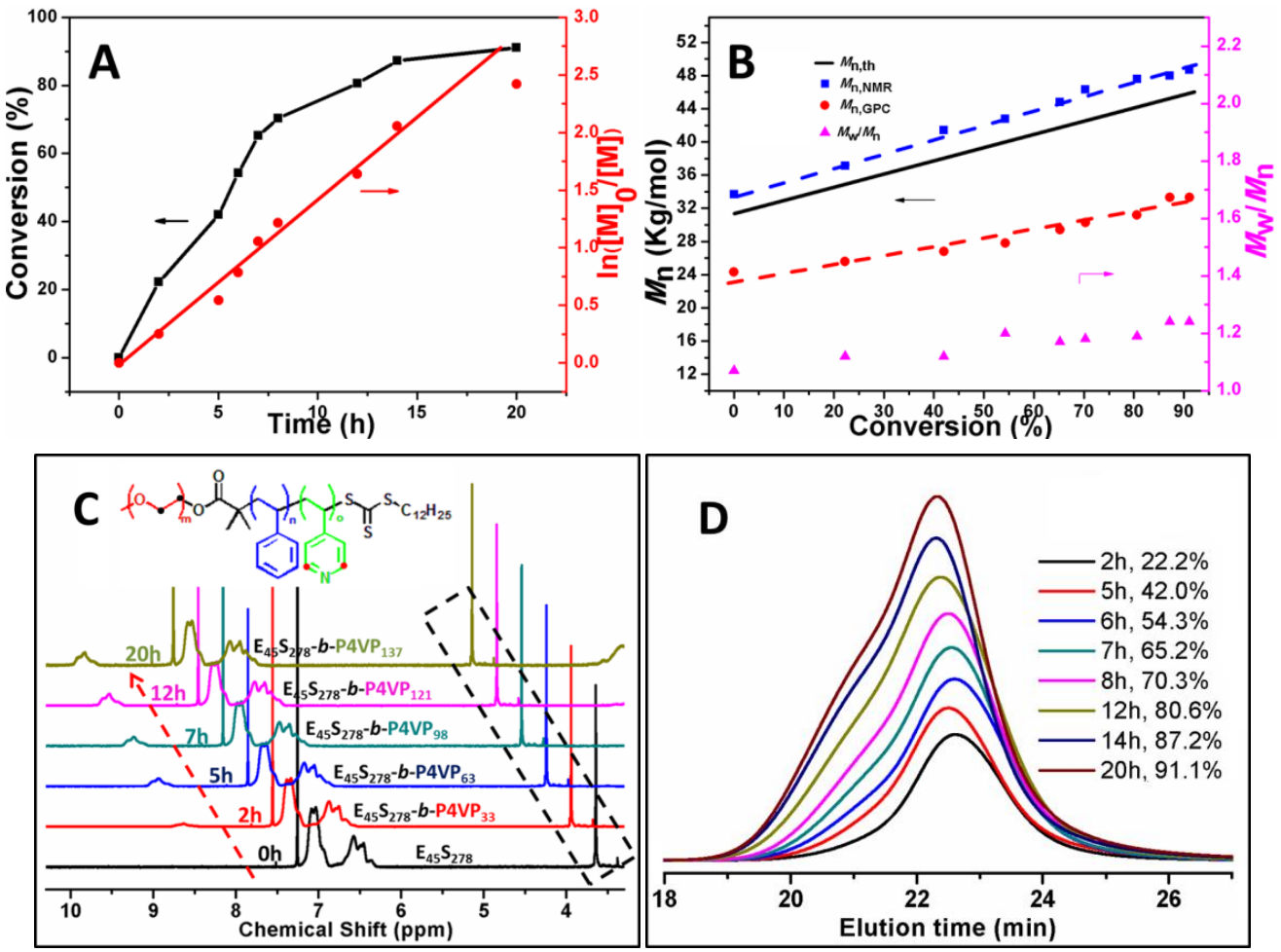

Figure 4. The monomer conversion-time plot and the ln([M]$_0$/[M])-time plot (A) for the seeded RAFT polymerization, the molecular weight and PDI (B), the ^{1}H NMR spectra (C), and the GPC traces (D) of the synthesized PEG_{45}-*b*-PS_{278}-*b*-P4VP triblock terpolymers. Polymerization conditions: 4VP (0.300 g, 2.86 mmol), the methanol/water mixture (3.38 g, 80/20 by weight), $[4VP]_0$:[PEG-*b*-PS-$TTC]_0$:$[AIBN]_0$ = 450:3:1, 70 ℃.

Polymer Chemistry Accepted Manuscript

This journal is © The Royal Society of Chemistry 2012

The kinetics of the seeded RAFT polymerization is summarized in Figure 4A. The monomer conversion increases with the polymerization time and finally reaches to 91.1% in 20 h. The further increase in the polymerization time just leads to a very slight increase in the monomer conversion. From the linear $\ln([M]_0/[M])$-time plot, the pseudo-first order kinetics of the seeded RAFT polymerization just like a general homogeneous RAFT polymerization is concluded.[55] The PEG_{45}-*b*-PS_{278}-*b*-P4VP triblock terpolymers synthesized at different polymerization times are characterized by ^{1}H NMR analysis (Figure 4C) and GPC analysis (Figure 4D). From the ^{1}H NMR spectra shown in Figure 4C, the increasing signal at δ = 8.32 ppm corresponding to the pyridine group in the P4VP block as indicated out by red arrow with the polymerization time is detected, indicating the chain extension of the P4VP block in the PEG_{45}-*b*-PS_{278}-*b*-P4VP triblock terpolymer during the RAFT polymerization. The molecular weight $M_{n,NMR}$ of the triblock terpolymer is calculated by comparing the area ratio of the characteristic chemical shift at δ = 8.32 ppm corresponding to the pyridine group in the P4VP block to that of the protons at δ = 3.64 ppm corresponding to the PEG block, and the results are summarized in Figure 4B. As shown in the GPC traces, slight shoulder at the high molecular weight side is observed, suggesting slight bimolecular radical termination in the seeded RAFT polymerization as indicated by the moderate PDI values locating at 1.1-1.3. As summarized in Figure 4B, the molecular weight of the PEG_{45}-*b*-PS_{278}-*b*-P4VP triblock terpolymers, whether $M_{n,NMR}$ by ^{1}H NMR analysis or $M_{n,GPC}$ by GPC analysis, increases linearly with the monomer conversion, which is just like those in a homogeneous RAFT polymerization.[55] The theoretical molecular weight $M_{n,th}$ of the PEG_{45}-*b*-PS_{278}-*b*-P4VP triblock terpolymers is calculated by the monomer conversion following equation 1. It is found that $M_{n,NMR}$ and $M_{n,th}$ of the triblock terpolymer are close to each other, and both of them are higher than $M_{n,GPC}$. Note: see the detail of the PEG_{45}-*b*-PS_{278}-*b*-P4VP triblock terpolymers in Table S1. The underestimation of $M_{n,GPC}$ is possibly due to the hydrophobic PS standards used in the GPC analysis and the interaction of the N-containing block copolymer with the GPC columns,[56] which is also deemed to be correlative to the unsymmetrical GPC traces shown in Figure 4D.

The *in-situ* synthesized PEG-*b*-PS-*b*-P4VP triblock terpolymer nano-objects prepared at different polymerization times were checked by DLS analysis. As shown in Figure S1, the hydrodynamic diameter (D_h) of the PEG-*b*-PS-*b*-P4VP nano-objects increases from 158 to 246 nm, when the DP of the newly formed P4VP block increases from 0 to 131. It is deemed that two reasons are ascribed to the increasing D_h of the PEG-*b*-PS-*b*-P4VP nano-objects with the DP of the P4VP block. First, the P4VP chain length extends with the increasing DP of the P4VP block. Second, since the P4VP block is soluble in the 80/20 methanol/water mixture, the solvophilic P4VP chains will make the PEG-*b*-PS-*b*-P4VP nano-objects swollen in the solvent.

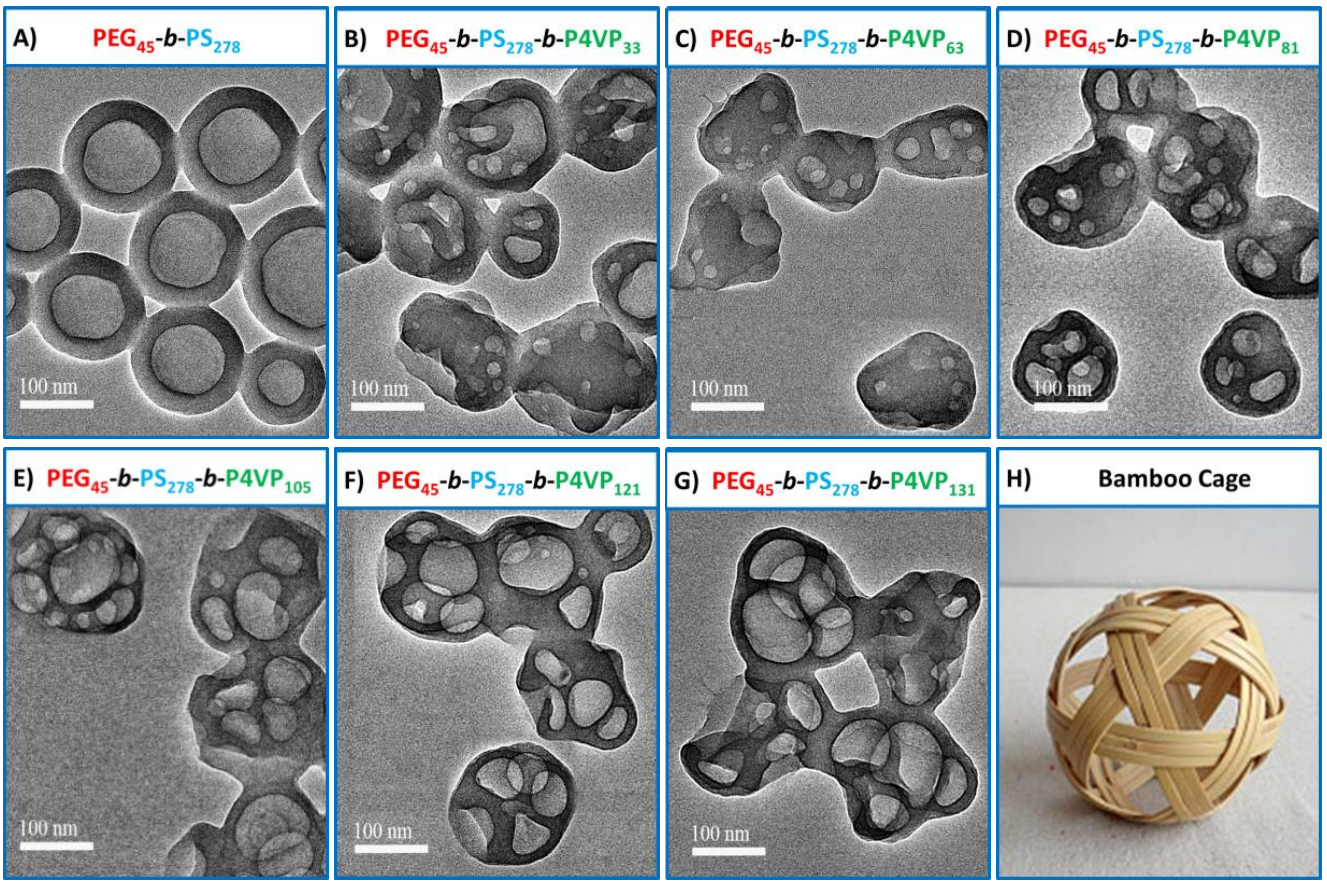

Figure 5. TEM images of the PEG_{45}-*b*-PS_{278}-TTC vesicles (A), the MCVs of PEG_{45}-*b*-PS_{278}-*b*-P4VP prepared at the polymerization time of 2 h (B), 5 h (C), 6 h (D), 8 h (E), 12 h (F), 14 h (G), and a real bamboo artwork (H).

Polymer Chemistry Accepted Manuscript

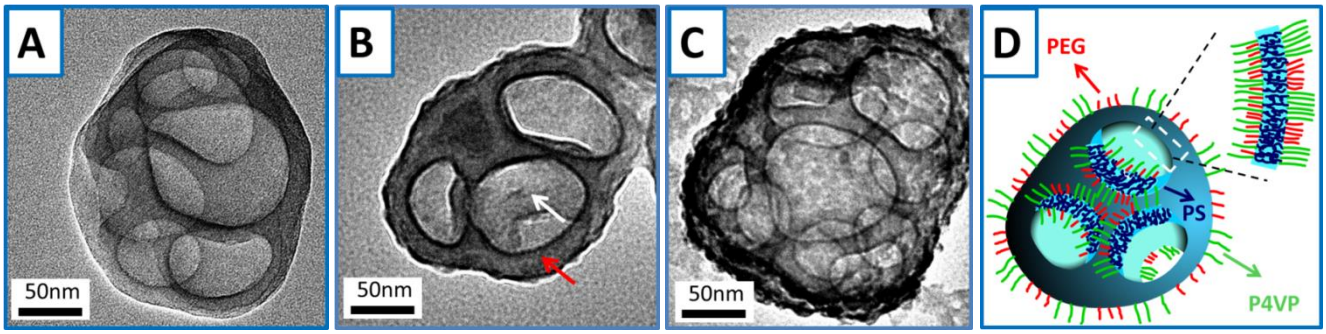

Figure 6. The TEM images of the typical PEG_{45}-*b*-PS_{278}-*b*-$P4VP_{105}$ MCVs dispersed in water: unstained MCVs (A), MCVs stained by I_2 vapor (B), MCVs stained jointly by PTA and I_2 vapor (C), and the schematic structure of the MCVs of PEG_{45}-*b*-PS_{278}-*b*-$P4VP_{105}$ (D).

The morphology of the PEG_{45}-*b*-PS_{278}-*b*-P4VP triblock terpolymer nano-objects at different polymerization times is checked. From the TEM images shown in Figure 5, it is found that the PEG_{45}-*b*-PS_{278}-TTC vesicles (Figure 5A) are converted into the membrane-compartmentalized vesicles (MCVs) (Figure 5B-5G), as indicated by the pores embedded within the membrane. The name of the MCVs is called, since the membrane is somehow segregated by the pores, which makes the MCVs look like a real cage (Figure 5H). As shown in Figure 5, the size of the MCVs is similar with that of the PEG_{45}-*b*-PS_{278}-TTC vesicles, whereas the pores embedded within the membrane increases with the DP of the P4VP block. Note: the DP of the P4VP block is kept below 150, since insertion a much long P4VP will disassemble the vesicles as discussed elsewhere.[47] The exact reason why the PEG_{45}-*b*-PS_{278}-TTC vesicles are converted into membrane-compartmentalized vesicles when a third solvophilic P4VP block is inserted in the vesicle membrane needs further study. It is supposed that the newly inserted P4VP increases the interfacial curvature of the membrane, which makes the membrane to be deformed. Furthermore, since the PS membrane is kinetically frozen by the solvent of the 80/20 methanol/water, the membrane deformation is somewhat restricted, and therefore the membrane is just segregated with pores to balance the increasing interfacial curvature.

The present MCVs are different from the general block copolymer vesicles reported previously,[4-12] and the detailed structure of the typical MCVs of PEG_{45}-*b*-PS_{278}-*b*-$P4VP_{105}$ is investigated by TEM. Figures 6A, B and C shows the TEM images of the unstained MCVs dispersed in water, MCVs stained by I_2 vapor and MCVs stained jointly by PTA and I_2 vapor, respectively. Note: the P4VP block in the MCVs becomes insoluble in water and therefore can be detected by TEM with the help of the staining chemicals, and I_2 vapor can selectively stain the P4VP phase as discussed elsewhere,[57] and the jointed staining initially with phosphotungstic acid and then with I_2 helps to clearly discern the P4VP phase on MCVs. By comparing Figure 6A with Figure 6B, it is found that the inner side and outer side of the membrane, which are indicated out by a white arrow and a red arrow, respectively, are slightly different. That is, the inner membrane and the outer membrane are studded with the black island-like dots of the P4VP phase, which is further confirmed by the TEM image shown in Figure 6C. This suggests that the P4VP chains are uniformly distributed in the inner side of the membrane, whereas at the outer side of the membrane, several P4VP chains are converged together and were segregated by the neighbouring PEG chains as schematically shown in Figure 6D, since the uniformly distributed P4VP chains tend to form the continuous P4VP phase and whereas the segregated and converged P4VP chains tend to form dispersed island-like P4VP phase in water. Note: the distribution of the PEG chains at the outer and inner sides of the membrane cannot be detected, and they are deemed to be distributed at the outer and inner sides of the membrane.

4 Conclusions

Diblock copolymer vesicles of PEG_{45}-*b*-PS_{278}-TTC were prepared, and modification of the PEG_{45}-*b*-PS_{278}-TTC vesicles by seeded RAFT polymerization was investigated. Through the PEG_{45}-TTC macro-RAFT agent mediated dispersion polymerization, well defined PEG_{45}-*b*-PS_{278}-TTC vesicles with the membrane thickness at 27±3 nm were prepared. Modification of the PEG_{45}-*b*-PS_{278}-TTC vesicles by the extension of the third solvophilic P4VP block through seeded RAFT polymerization was achieved. It was found, during the seeded RAFT polymerization, the PEG-*b*-PS-TTC diblock copolymer was extended to the PEG-*b*-PS-*b*-P4VP triblock terpolymer, and the PEG-*b*-PS-TTC vesicles were converted into membrane-compartmentalized vesicles (MCVs), in which the membrane was deformed and was segregated by pores. It was found that the membrane structure of MCVs was correlative to the DP of the P4VP chains. The P4VP chains were found to be uniformly distributed in the inner side of the membrane, whereas at the outer side of the membrane, several P4VP chains were converged together and were segregated by the neighbouring PEG chains. The proposed seeded RAFT polymerization may be a promising method of vesicle modification, and the MCVs with segregated membrane structure are deemed to be a new morphology of the triblock terpolymer nano-assemblies.

Acknowledgements

The financial support by National Science Foundation of China (№ 21274066 and 21474054) and PCSIRT (IRT1257) is gratefully acknowledged.

Notes and references

[a] MOE Key Laboratory of Wooden Material Science and Application, Beijing Forestry University, Beijing 100083, China.

Polymer Chemistry Accepted Manuscript

 This journal is © The Royal Society of Chemistry 2012

[b] Key Laboratory of Functional Polymer Materials of the Ministry of Education, Collaborative Innovation Center of Chemical Science and Engineering (Tianjin), Institute of Polymer Chemistry, Nankai University, Tianjin 300071, China.

Electronic Supplementary Information (ESI) available: Table S1 summarizing the PEG-*b*-PS-*b*-P4VP triblock terpolymer and Figure S1 showing the hydrodynamic diameter (D_h) distribution of the PEG-*b*-PS-*b*-P4VP nano-objects. See DOI: 10.1039/b000000x/.

1 J. Du and R. K. O'Reilly, *Soft Matter*, 2009, **5**, 3544-3561.
2 G. Battaglia and A. J. Ryan, *J. Am. Chem. Soc*., 2005, **127**, 8757-8764.
3 M. Semsarilar, V. Ladmiral, A. Blanazs and S. P. Armes, *Polym. Chem*., 2014, **5**, 3466-3475.
4 S. A. Meeuwissen, S. M. C. Bruekers, Y. Chen, D. J. Pochan and J. C. M. van Hest, *Polym. Chem*., 2014, **5**, 489-501.
5 J. del Barrio, L. Oriol, C. Sanchez, J. L. Serrano, A. D. Cicco, P. Keller and M.-H. Li, *J. Am. Chem. Soc*., 2010, **132**, 3762-3769.
6 A. E. Smith, X. Xu, S. E. Kirkland-York, D. A. Savin and C. L. McCormick, *Macromolecules*, 2010, **43**, 1210-1217.
7 Q.Yan, R. Zhou, C. Fu, H. Zhang, Y. Yin and J. Yuan, *Angew. Chem. Int.Ed*., 2011, **50**, 4923-4927.
8 G. Sun, H. Fang, C. Cheng, P. Lu, K. Zhang, A. V. Walker, J.-S. A. Taylor and K. L. Wooley, *ACS Nano*, 2009, **3**, 673-681.
9 R. Dong, B. Zhu, Y. Zhou, D. Yan and X. Zhu, *Angew. Chem. Int.Ed*., 2012, **51**, 11633-11637.
10 K. Rajagopal, A. Mahmud, D. A. Christian, J. D. Pajerowski, A. E. Brown, S. M. Loverde and D. E. Discher, *Macromolecules*, 2010**, 43**, 9736-9746.
11 J. Braun, N. Bruns, T. Pfohl and W. Meier, *Macromol. Chem. Phys*., **2011**, *212*, 1245-1254.
12 T. Azzam and A. Eisenberg, *Angew. Chem. Int. Ed*., 2006, **45**, 7443-7447.
13 S. Yu, T. Azzam, I. Rouiller and A. Eisenberg, *J. Am. Chem. Soc*.**,** 2009, **131**, 10557-10566.
14 A. Sundararaman, T. Stephan and R. B. Grubbs, *J. Am. Chem. Soc*., 2008, **130**, 12264-12265.
15 L. Zhang and A. Eisenberg, *Science*, 1995, **268**, 1728-1731.
16 C. Schwieger, A. Achilles, S. Schloz, J. Rüger, K. Bacia, K. Saalwaechter, J. Kressler and A. Blume, *Soft Matter*, 2014, **10**, 6147-6160.
17 C. Pietsch, U. Mansfeld, C. Guerrero-Sanchez, S. Hoeppener, A. Vollrath, M. Wagner, R. Hoogenboom, S. Saubern, S. H. Thang, C. R. Becer, J. Chiefari and U. S. Schubert, *Macromolecules*, 2012, **45**, 9292-9302.
18 P. Zou and C.-Y. Pan, *Macromol. Rapid Commun*., 2008, **29**, 763-771.
19 D. A. Christian, A. Tian, W. G. Ellenbroek, I. Levental, K. Rajagopal, P. A. Janmey, A. J. Liu, T. Baumgart and D. E. Discher, *Nature Mater*., 2009, **8**, 843-849.
20 H. Hu and G. Liu, *Macromolecules*, 2014, **47**, 5096-5103.
21 W. Zhao, D. Chen, Y. Hu, G. M. Grason and T. P. Russell, *ACS Nano*, 2011, **5**, 486-492.
22 A. Palanisamy and Q. Guo, *J. Phys. Chem. B*, 2014, **118**, 12796-12803.
23 M. J. Greenall, P. Schuetz, S. Furzeland, D. Atkins, D. M. A. Buzza, M. F. Butler and T. C. B. McLeish, *Macromolecules*, 2011, **44**, 5510-5519.
24 M. J. Monteiro, M. Hodgson and H. De Brouwer, *J. Polym. Sci. Part A: Polym. Chem*., 2000, **38**, 3864-3874.
25 W. Zhang, F. D'Agosto, O. Boyron, J. Rieger and B. Charleux, *Macromolecules*, 2012, **45**, 4075-4084.
26 G. Delaittre, C. Dire, J. Rieger, J.-L. Putaux and B. Charleux, *Chem. Commun*., 2009, **20**, 2887-2889.
27 C. Gonzato, M. Semsarilar, E. R. Jones, F. Li, G. J. P. Krooshof, P. Wyman, O. O. Mykhaylyk, R. Tuinier and S. P. Armes, *J. Am. Chem. Soc*., 2014, **136**, 11100-11106.
28 X. Zhang, S. Boissé, C. Bui, P.-A. Albouy, A. Brûlet, M.-H. Li, J. Rieger and B. Charleux, *Soft Matter*, 2012, **8**, 1130-1141.
29 N. J. Warren, O. O. Mykhaylyk, D. Mahmood, A. J. Ryan and S. P. Armes, *J. Am. Chem. Soc*., 2014, **136**, 1023-1033.
30 N. J. Warren and S. P. Armes, *J Am Chem Soc*., 2014, **136**, 10174-10185.
31 Y. Pei, L. Thurairajah, O. R. Sugita and A. B. Lowe, *Macromolecules*, 2015, **48**, 236-244.
32 Y. Pei and A. B. Lowe, *Polym. Chem*., 2014, **5**, 2342-2351.
33 W.-D. He, X.-L. Sun, W.-M. Wan and C.-Y. Pan, *Macromolecules*, 2011, **44**, 3358-3365.
34 W.-J. Zhang, C.-Y. Hong and C.-Y. Pan, *Macromolecules*, 2014, **47**, 1664-1671.
35 X. Xiao, S. He, M. Dan, Y. Su, F. Huo and W. Zhang, *J. Polym. Sci. Part A: Polym. Chem*., 2013, **51**, 3177-3190.
36 C. Gao, S. Li, Q. Li, P. Shi, S. A. Shah and W. Zhang, *Polym. Chem*., 2014, **5**, 6957-6966.
37 M. Antonietti and S. Förster, *Adv. Mater*., 2003, **15**, 1323-1333.
38 J. Israelachvili, *Intermolecular & Surface Forces*, 2nd ed, Academic Press: London, 1991.
39 G. Njikang, D. Han, J. Wang and G. Liu, *Macromolecules*, 2008, **41**, 9727-9735.
40 M. C. M. van Oers, F. P. J. T. Rutjes and J. C. M. van Hest, *J. Am. Chem. Soc*., 2013, **135**, 16308-16311.
41 Y. Han, H. Yu, H. Du and Jiang, W. *J. Am. Chem. Soc*., **2010**, *132*, 1144-1150.
42 E. V. Korchagina, X.-P. Qiu and F. M. Winnik, *Macromolecules*, 2013, **46**, 2341-2351.
43 H. Fan and Z. Jin, *Macromolecules*, 2014, **47**, 2674-2681.
44 M. Chenal, L. Bouteiller and J. Rieger, *Polym. Chem*., 2013, **4**, 752-762.
45 R. Wei, Y. Luo and Z. Li, *Polymer*, 2010, **51**, 3879-3886.
46 F. Huo, C. Gao, M. Dan, X. Xiao, Y. Su and W. Zhang, *Polym. Chem*., 2014, **5**, 2736-2746.
47 F. Huo, S. Li, X. He, S. A. Shah, Q. Li and W. Zhang, *Macromolecules*, *2014*, **47**, 8262-8269.
48 D. E. Ganeva, E. Sprong, H. de Bruyn, G. G. Warr, C. H. Such and B. S. Hawkett, *Macromolecules*, 2007, **40**, 6181-6189.
49 X. Xiao, S. He, M. Dan, F. Huo and W. Zhang, *Chem. Commun*., 2014, **50**, 3969-3972.
50 J. T. Lai, D. Filla and R. Shea, *Macromolecules*, 2002, **35**, 6754-6756.
51 Y. He and T. P. Lodge, *Macromolecules*, 2008, **41**, 167-174.
52 C. Gao, Q. Li, Y. Cui, F. Huo, S. Li, Y. Su, and Zhang, W. *J. Polym. Sci. Part A: Polym. Chem*., 2014, **52**, 2155-2165.
53 H. de Brouwer, M. A. J. Schellekens, B. Klumperman, M. J. Monteiro and A. L. German, *J. Polym. Sci. Part A: Polym. Chem*., 2000, **38**, 3596-3603.
54 Z. Li, J. Ma, C. Cheng, K. Zhang and K. L. Wooley, *Macromolecules*, 2010, **43**, 1182-1184.

Polymer Chemistry Accepted Manuscript

55 Z. Jia, X. Xu, Q. Fu and J. Huang, *J. Polym. Sci. Part A: Polym. Chem*., 2006, **44**, 6071-6082.
56 A. P. Narrainen, S. Pascual and D. M. Haddleton, *J. Polym. Sci. Part A: Polym. Chem*., 2002, **40**, 439-450.
57 V. Pale, T. Nikkonen, J. Vapaavuori, M. Kostiainen, J. Kavakka, J. Selin, I. Tittonen, and J. Helaja, *J. Mater. Chem. C*, 2013, **1**, 2166-2173.

Polymer Chemistry Accepted Manuscript

 This journal is © The Royal Society of Chemistry 2012